Asian Journal of Andrology (2021) 23, 197–204
www.asiaandro.com; www.ajandrology.com

Open Access

ORIGINAL ARTICLE

Male Infertility

A novel homozygous frameshift mutation in *MNS1* associated with severe oligoasthenoteratozoospermia in humans

Yong Li[1,*], Wei-Li Wang[1,*], Chao-Feng Tu[1,2,3], Lan-Lan Meng[2,3], Tong-Yao Hu[1], Juan Du[1,2,3], Ge Lin[1,2,3], Hong-Chuan Nie[1,2,3], Yue-Qiu Tan[1,2,3]

Oligoasthenoteratozoospermia (OAT) refers to the combination of various sperm abnormalities, including a decreased sperm count, reduced motility, and abnormal sperm morphology. Only a few genetic causes have been shown to be associated with OAT. Herein, we identified a novel homozygous frameshift mutation in meiosis-specific nuclear structural 1 (*MNS1*; NM_018365: c.603_604insG: p.Lys202Glufs*6) by whole-exome sequencing in an OAT proband from a consanguineous Chinese family. Subsequent variant screening identified four additional heterozygous *MNS1* variants in 6/219 infertile individuals with oligoasthenospermia, but no *MNS1* variants were observed among 223 fertile controls. Immunostaining analysis showed MNS1 to be normally located in the whole-sperm flagella, but was absent in the proband's sperm. Expression analysis by Western blot also confirmed that MNS1 was absent in the proband's sperm. Abnormal flagellum morphology and ultrastructural disturbances in outer doublet microtubules were observed in the proband's sperm. A total of three intracytoplasmic sperm injection cycles were carried out for the proband's wife, but they all failed to lead to a successful pregnancy. Overall, this is the first study to report a loss-of-function mutation in *MNS1* causing OAT in a Han Chinese patient.
Asian Journal of Andrology (2021) **23**, 197–204; doi: 10.4103/aja.aja_56_20; published online: 02 October 2020

Keywords: intracytoplasmic sperm injection; male infertility; meiosis-specific nuclear structural 1 (*MNS1*) ; oligoasthenoteratozoospermia; whole-exome sequencing

INTRODUCTION

Infertility is a significant global health issue that affects approximately 15% of couples, with male factors and female factors contributing equally.[1] Infertile men frequently exhibit sperm abnormalities, which could be identified through conventional semen analysis. According to the World Health Organization (WHO) guidelines,[2] semen analysis may show decreased sperm count (oligozoospermia, the sperm count $<15 \times 10^6$ ml^{-1}), poor motility (asthenozoospermia, progressive sperm <32%), and abnormal sperm morphology (teratozoospermia, amount of morphologically normal sperm <4%). The combination of these abnormalities is termed oligoasthenoteratozoospermia (OAT),[3] and idiopathic OAT (iOAT) is responsible for approximately 30% of all cases of male infertility.[4] Recently, a specific kind of asthenoteratozoospermia, the multiple morphological abnormalities of the sperm flagella (MMAF), has been identified and is characterized by various flagellar morphological abnormalities (absent, short, bent, coiled, and irregular flagella).[5]

The etiology of male infertility is extremely complicated, and the causes remain largely unknown.[6] It is currently thought that genetic defects account for at least 15% of all male infertility cases.[7] More than 2300 genes have been predicted to be involved in spermatogenesis,[8] but causal mutations have only been identified in a small number of genes in humans. To date, only a few genes associated with OAT have been identified including FA complementation group M (*FANCM*),[9] dynein axonemal heavy chain 1 (*DNAH1*),[5] and cilia- and flagella-associated protein 44 (*CFAP44*)[9,10] in humans and acetylgalactosaminyltransferase 3 (*Galnt3*),[11] CCR4-NOT transcription complex subunit 7 (*Cnot7*),[12] HIV-1 rev-binding protein (*Hrb*),[13] cell adhesion molecule 1 (*Cadm1*/*Ra175*),[14] and oxysterol-binding protein-related protein 4 (*Orp4*)[15] in mice. The majority of genetic causes and associated mechanisms of OAT in humans still remain unclear.

MNS1, meiosis-specific nuclear structural 1, is located at 15q21.3 in humans and has 10 exons encoding a 495-amino acid protein, which has been identified in human bronchial epithelium.[16] *Mns1* was found to be essential for sperm tail development in mice, and *Mns1*-knockout (KO) mice present with male infertility due to OAT.[17] In humans, three homozygous loss-of-function mutations in *MNS1* from two unrelated groups have been reported to potentially cause laterality defects and male infertility.[18,19] However, the explicit infertility phenotype caused by mutations in *MNS1* is poorly understood.

In this study, we performed whole-exome sequencing (WES) in an idiopathic infertile male with severe OAT from a consanguineous family. A homozygous loss-of-function mutation in *MNS1* was identified and functionally characterized using the patient's

[1]Institute of Reproductive and Stem Cell Engineering, School of Basic Medical Science, Central South University, Changsha 410078, China; [2]Reproductive and Genetic Hospital of CITIC-Xiangya, Changsha 410078, China; [3]Clinical Research Center for Reproduction and Genetics in Hunan Province, Changsha 410078, China.
*These authors contributed equally to this work.
Correspondence: Dr. YQ Tan (tanyueqiu@csu.edu.cn) or Dr. HC Nie (doctornie@qq.com)
Received: 21 October 2019; Accepted: 14 July 2020

spermatozoa. This is the first report of an *MNS1* mutation associated with OAT in a Chinese patient.

PATIENTS AND METHODS

Patients

The proband (family member IV-1, 34 years old) with primary infertility from a consanguineous Han Chinese family (Changde, China) visited the Reproductive and Genetic Hospital of CITIC-Xiangya for genetic counseling of infertility treatment. Although the couple had been married for 7 years, his wife failed to conceive in the absence of contraception. The proband's wife (33 years old) did not show any abnormities upon routine clinical examination before intracytoplasmic sperm injection (ICSI) treatment. The proband's parents (III-1 and III-2) were first-degree cousins from Hunan province. In addition, the proband's brother (IV-2) is fertile and his wife gave birth to a child through normal delivery. Written informed consent was obtained from all the participants in this study. This study was approved by the Ethics Committee (Changsha, China) of the Reproductive and Genetic Hospital of CITIC-Xiangya and Central South University (LL-SC-2017-025).

Whole-exome sequencing

Peripheral blood samples of the family members (III-1, III-2, IV-1, and IV-2) were collected. Genomic DNA samples from peripheral blood were extracted using a QIAamp DNA Blood Midi Kit (Qiagen, Hilden, Germany). The proband (IV-1) was subjected to WES using the HiSeq 2000 sequencing platform (Illumina, San Diego, CA, USA) at the Beijing Genome Institute in Shenzhen. Agilent SureSelect Human All Exon v6 Kit (Agilent, Santa Clara, CA, USA) was used for the capture of known exons and exon–intron boundary sequences. The detailed procedure of WES and the data analysis conducted have been described previously.[20]

Bioinformatics and in silico analysis of the candidate variant

The putative gene pathogenic variants that matched the following criteria were considered: (1) allele frequencies below 5% in the following databases (dbSNP, 1000 Genomes Project, ExAC); (2) the variations were predicted to be deleterious using four different tools: polyphen-2 (http://genetics.bwh.harvard.edu/pph2), SIFT (http://sift.bii.a-star.edu.sg/), Mutation Taster (http://www.mutationtaster.org/), and Combined Annotation-Dependent Depletion (CADD; cadd.gs.washington.edu/); (3) highly expressed in testes; and (4) associated with fertility. Homozygosity mapping was performed using HomozygosityMapper,[21] and homozygous variants located in homozygous regions >2.0 Mb were prioritized. For *in silico* analysis, evolutionary conservation analysis was performed through alignment of the amino acid sequences of the proteins between different species from the GenBank database (https://www.ncbi.nlm.nih.gov/homologene/). The protein structure was predicted using the simple modular architecture research tool (SMART) database (http://smart.embl-heidelberg.de/).

Sanger sequencing

The candidate variant of *MNS1* was validated by Sanger sequencing using specific primers flanking the variant of the candidate gene, *MNS1*-F: 5'-GAAACGTGATGCTGAAATAGCC-3' and *MNS1*-R: 5'-AGTTCCTCACAACAAACCTGTGATA-3'. The variant site in *MNS1* was amplified through polymerase chain reaction (PCR) using Ex Taq DNA polymerase (Bio-Rad, Hercules, CA, USA) for all the family members. All the PCR products were sequenced using the ABI 3730 automated sequencer (Applied Biosystems, Foster City, CA, USA) according to the manufacturer's instructions.

Hematoxylin and eosin (H&E) staining and immunostaining

To obtain the sperm smears, sperm from the proband and the fertile control individual were washed using a saline solution, centrifuged, smeared, and fixed in 4% paraformaldehyde (PFA). In order to visualize the morphological features of sperm, sperm smears were stained with H&E. Immunostaining of the slides was performed as described previously.[22] Sperm smears were incubated with primary antibodies: MNS1, A-kinase anchoring protein 4 (AKAP4, a fibrous sheath marker),[23] translocase of outer mitochondrial membrane 20 (TOMM20, a mitochondrial sheath marker),[24] dynein axonemal intermediate chain 1 (DNAI1, an outer dynein arms marker),[25,26] dynein axonemal light intermediate chain 1 (DNALI1, an inner dynein arms marker),[27] and anti-acetylated tubulin monoclonal antibody for 2 h at 37°C. The details of the antibodies are listed in **Supplementary Table 1**. The binding of the antibodies was detected by incubating with Alexa Fluor 488 anti-mouse IgG (A-21121; Invitrogen, Carlsbad, CA, USA; 1:400) and Alexa Fluor 555 anti-rabbit IgG (A31572; Invitrogen; 1:400) for 1 h at 37°C. Subsequently, the sperm smears were stained with 4',6-diamidino-2-phenylindole (DAPI) for 5 min. Finally, they were viewed using an Olympus BX-51 fluorescence microscope (Olympus, Tokyo, Japan).

Transmission electron microscopy (TEM)

Sperm of the proband and the fertile control individual were fixed overnight in 2.5% glutaraldehyde (Sigma-Aldrich, Saint Louis, MO, USA) in 0.1 mol l^{-1} phosphate buffer (pH 7.4), and then in 1.0% osmium tetroxide (OsO_4, HalingBio, Shanghai, China) for 2 h. They were immediately subjected to postfixation processing with 1% OsO_4 and 0.1 mol l^{-1} sucrose in 0.1 mol l^{-1} phosphate buffer; subsequently dehydrated with graded concentrations of ethanol; and thereafter embedded in Epon812, dodecenylsuccinic anhydride, methylnadic anhydride, and dimethylaminomethyl phenol (EMS, Hatfield, PA, USA) at 60°C for 24 h. Semithin 1-μm-thick sections were stained with toluidine blue (Solarbio, Beijing, China) for light microscopy (Olympus). Ultrathin 80 nm-thick sections were contrasted with uranyl acetate (Chemos, Altdorf, Germany) and lead citrate (Chemos) and examined using a H7700 Hitachi electron microscope (Hitachi, Tokyo, Japan). Digital images were captured using a MegaView III digital camera (MegaView, Munster, Germany).

Western blot

Western blot analysis of proteins in the sperm was performed as described previously.[22] Briefly, proteins of the proband and control individual were blotted onto a polyvinylidene difluoride membrane and incubated overnight at 4°C with anti-MNS1 antibody (Sigma-Aldrich, HPA039975). The samples were then incubated with goat anti-rabbit IgG-horseradish peroxidase-conjugated secondary antibodies (GAR007-100, Multi Sciences, Hangzhou, China) and visualized by enhanced chemiluminescence (Pierced, Grand Island, NY, USA). Glyceraldehyde 3-phosphate dehydrogenase (GAPDH) was used as the control.

Population screening for MNS1 variants

Peripheral blood genomic DNA samples were collected from 219 infertile individuals with oligoasthenospermia and 223 fertile controls who had normal fertility and at least one live offspring via natural fertilization. All the infertile individuals and the fertile controls were of Han Chinese origin. Following WHO guidelines (2010),[28] semen volume, sperm count, sperm progressive motility, and proportion of normal morphology of all the infertile individuals and the fertile controls were evaluated (**Table 1**). All the DNA samples were

subjected to WES and Sanger sequencing as previously described[29] (**Supplementary Table 2**). Neither abnormal somatic karyotypes nor Y chromosome microdeletions were detected.

RESULTS

Clinical characterization of the proband

The proband (IV-1) was 34 years old and from a consanguineous family (**Figure 1a**). The semen examination results of the proband were as follows: semen volume, 3.4 ml; sperm concentration, 1.8×10^6 ml^{-1}; and percentage progressive motility, 5.8%. Semen analysis revealed the normal sperm morphology to be 2.6% (**Table 1**). Collectively, these results led to the diagnosis of severe OAT. Physical examination results of the proband showed normal testicular size, external genital development, and bilateral spermatic vein. The chromosomal karyotype of the proband was 46,XY; no Y chromosome microdeletions were found. According to previous medical records of the proband, he had no history of respiratory disorders, situs inversus, exposure to hazardous environments, or poor habits such as smoking and drinking.

Identification of the MNS1 variant

WES was performed to determine the genetic causes of OAT in the proband. To identify likely pathogenic variants, those that occurred with a frequency of >5% in three public databases and predicted not to be deleterious were excluded; for patients from a consanguineous family, homozygous variants with known roles associated with the observed infertility phenotype or homozygous region larger than 2.0 Mb were prioritized. After screening, only one novel homozygous frameshift variant (NM_018365: exon5: c.603_604insG: p.Lys202Glufs*6) in *MNS1* was found to fulfill

Table 1: Semen analysis and intracytoplasmic sperm injection treatment of the proband IV-1 and screened individuals

Patient	*Age (year)*	*Semen volume (ml)*	*Sperm concentration (10^6 ml^{-1})*	*Progressive motile (%)*	*Normal morphology (%)*	*Wife's age (year)*	*Number of MII oocytes (n)*	*Normal fertilization (n)*	*Number of embryos transferred (n)*	*Clinical pregnancy (n)*	*Ongoing pregnancy (n)*
Control individuals[a]	NA	>1.4	>15	>32	>4	NA	NA	NA	NA	NA	NA
IV-1	34	3.4	1.8	5.8	2.6	33	10	8	2	0	0
P1	30	3.4	4.3	30.3	2.5	27	10	8	2	0	0
P2	33	4.3	2.6	5.7	2.8	34	12	9	2	1	1
P3	28	4.5	2.2	9.9	2.5	27	6	4	NA	NA	NA
P4	29	2.8	3.4	8.9	2.5	34	2	2	2	1	0
P5	36	4.3	4.2	17.1	2.5	36	13	11	2	0	0
P6	27	4.1	0.8	6.3	1.0	25	NA	NA	NA	NA	NA

[a]World Health Organization ranges for semen parameters in normal individuals. ICSI: intracytoplasmic sperm injection; NA: not applicable

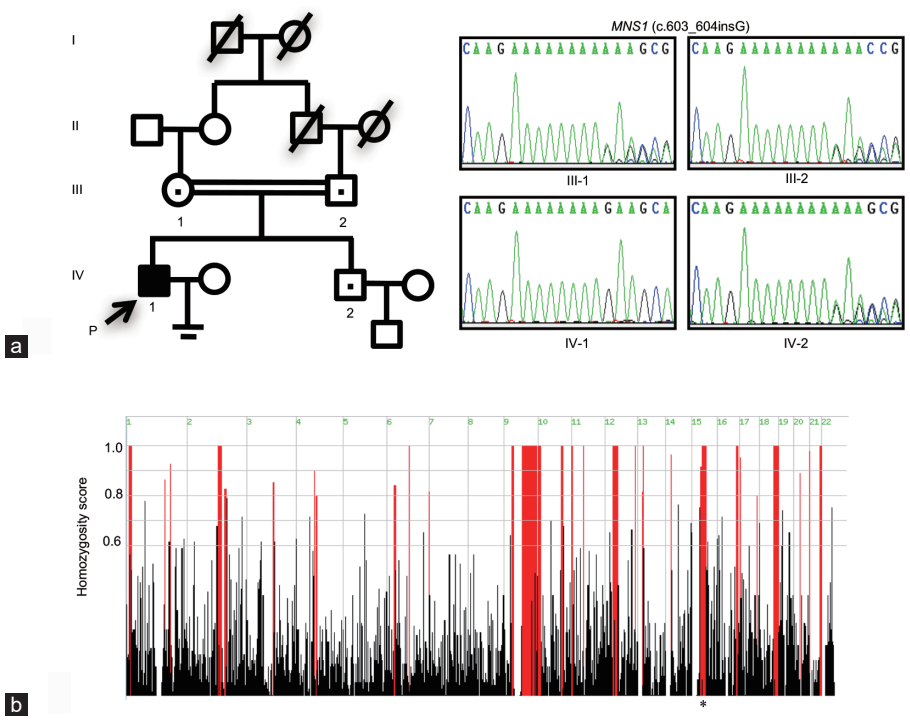

Figure 1: Pedigree of the family and analyses of *MNS1* in the consanguineous Chinese family. (**a**) The pedigree of the consanguineous Chinese family with inherited *MNS1* pathogenic variant. The proband in these families is indicated as "P" plus a black arrow. A dot in the middle of the symbol indicates heterozygous carriers. Sanger sequencing confirmation of *MNS1* variant c.603_604insG in this family; the unaffected parents and the proband's brother are heterozygous carriers of the variation of *MNS1*, c.603_604insG, whereas the proband is homozygous for the variation. (**b**) Homozygosity mapping of the proband. Homozygous regions with remarkable signal are indicated in red. The asterisk indicates the area where *MNS1* is located. P: proband; *MNS1*: meiosis-specific nuclear structural 1.

these criteria (**Figure 1b** and **Table 2**). However, this variant was absent in public databases (**Table 2**). Subsequent Sanger sequencing and co-segregation analysis confirmed that the proband was homozygous for the variant, whereas the unaffected proband's parents and brother were heterozygous carriers (**Figure 1a**). The gene variant co-segregated with the OAT phenotype in the family and is also consistent with the autosomal recessive mode of inheritance. No apparent deleterious biallelic variants in *MNS1* were found in 219 infertile individuals with oligoasthenospermia and 223 fertile controls from the Han Chinese population. Although four *MNS1* heterozygous variants in six infertile individuals with oligoasthenospermia (none in the fertile control; **Table 2** and **Supplementary Figure 1a**) were identified, they were unlikely to be the cause of infertility for these infertile individuals. Thus, other candidate variants in other genes should be investigated in future.

The impact of MNS1 variant

Evolutionary conservation analysis showed that the amino acid (lysine 202) in human MNS1 is highly conserved among different species (**Figure 2a**), revealing the functional importance of the lysine 202 site. The frameshift variant occurred in the fifth exon (**Figure 2b**) and was predicted to result in a premature termination codon (PTC) at site 207. The PTC could involve nonsense-mediated mRNA decay (NMD), leading to the absence of MNS1 protein or generation of a truncated protein (206 amino acids), which might maintain partial functionality or totally degrade due to instability.

To identify the exact impact of the *MNS1* frameshift variant, we explored the expression of *MNS1* in the proband. Western blot analysis was performed for the sperm proteins using the C-terminus antibody (binding 368–488 aa). The fertile control showed a band of MNS1 at approximately 60 kDa, but the same was absent in the proband's sperm (**Figure 2c**). Because the mutated transcript is almost certainly a substrate for NMD, it is probable that MNS1 was absent from the flagella in the proband. Immunostaining also showed that MNS1 was located in the whole-length sperm flagella of the control individual, but was absent in the proband's sperm (n = 120; **Figure 2d** and **Supplementary Figure 2a**). Collectively, these results strongly suggest that the *MNS1* frameshift mutation is the cause of OAT in the proband.

Sperm morphology and structural defects

H&E staining and TEM were performed to reveal the abnormalities of sperm morphology and ultrastructure. Although there were also some spermatozoa with seemingly normal morphology, H&E staining showed that there were morphological abnormalities in the proband's sperm, including absent, bent, coiled, and short flagella, compared to the control individual (**Figure 3a**). The absent, bent, coiled, and short flagella, respectively, accounted for 15.0%, 20.0%, 29.2%, and 32.5% in the proband's sperm (n = 120; **Table 3**). TEM showed ultrastructural defects in the proband's sperm, with frequent absence of outer doublet microtubules (DMT, 7 + 2, 6 + 2, or 5 + 2, accounting for 40%), and sporadic absence of the central complex (6 + 0 or 9 + 0, accounting for 8%) in 50% (n = 50) of the cross-sections, compared to the normal control (**Figure 3b**). To further determine abnormalities in the axonemal or peri-axonemal structures of the sperm flagella in the proband, immunostaining was performed. For each marker, ≥100 sperm were analyzed for both the proband and the normal control. In the proband's spermatozoa, the staining signal of the outer dynein arms (ODA; DNAI1)[25,26] was undetectable compared to the normal control (**Figure 3c** and **Supplementary Figure 2b**), indicating that *MNS1* mutation induced a loss of ODAs in the sperm. Moreover, the

Table 2: Information for the identified *MNS1* variants in the proband IV-1 and screened subjects

Patient	*Variant location (GRCh37/hg19)*	*RefSeq ID*	*Variant*	*Exon*	*Amino acid change*	*Function*	*Zygosity*	*PolyPhen-2*[a]	*SIFT*[b]	*Mutation Taster*[c]	*CADD*	*ExAC*	*1000G*	*GnomADed*	*ExAC_ Asian*	*1000G_n Asian*	*GnomADe_ Asian*
IV-1	chr15: 56736724-56736724		c. 603_604insG	5	p.Lys202 Glufs*6	Frameshift	Homozygous	NA	NA	NA	NA	NA	NA	NA	NA	NA	NA
P1/P2	chr15: 56756300-56756300		c.G149A	2	p.Arg50 His	Nonsynonymous	Heterozygous	D	D	P	20	0.00001	0.000	0.00000	0.0000	0.000	0.000
P3/P4	chr15: 56739041-56739041	NM_018365	c.A454G	4	p.Met152 Val	Nonsynonymous	Heterozygous	B	T	D	22.7	0.00017	0.001	0.00020	0.0008	0.006	0.0010
P5	chr15: 56735891-56735893		c.846_848del	6	p.Glu282 del	Nonframeshift deletion	Heterozygous	NA	NA	D	NA	0.00003	NA	0.00004	0.0001	NA	0.0001
P6	chr15: 56735707-56735707		c.G932A	7	p.Arg311 Gly	Nonsynonymous	Heterozygous	B	T	D	21.4	0.00011	0.001	0.00012	0.0003	0.000	0.0004

[a]D: probably damaging; B: benign. [b]D: deleterious; T: tolerated. [c]P: polymorphism automatic; D: disease causing. [d]GnomAD-exomes. *MNS1*: meiosis-specific nuclear structural 1; NA: not available; CADD: Combined Annotation-Dependent Depletion

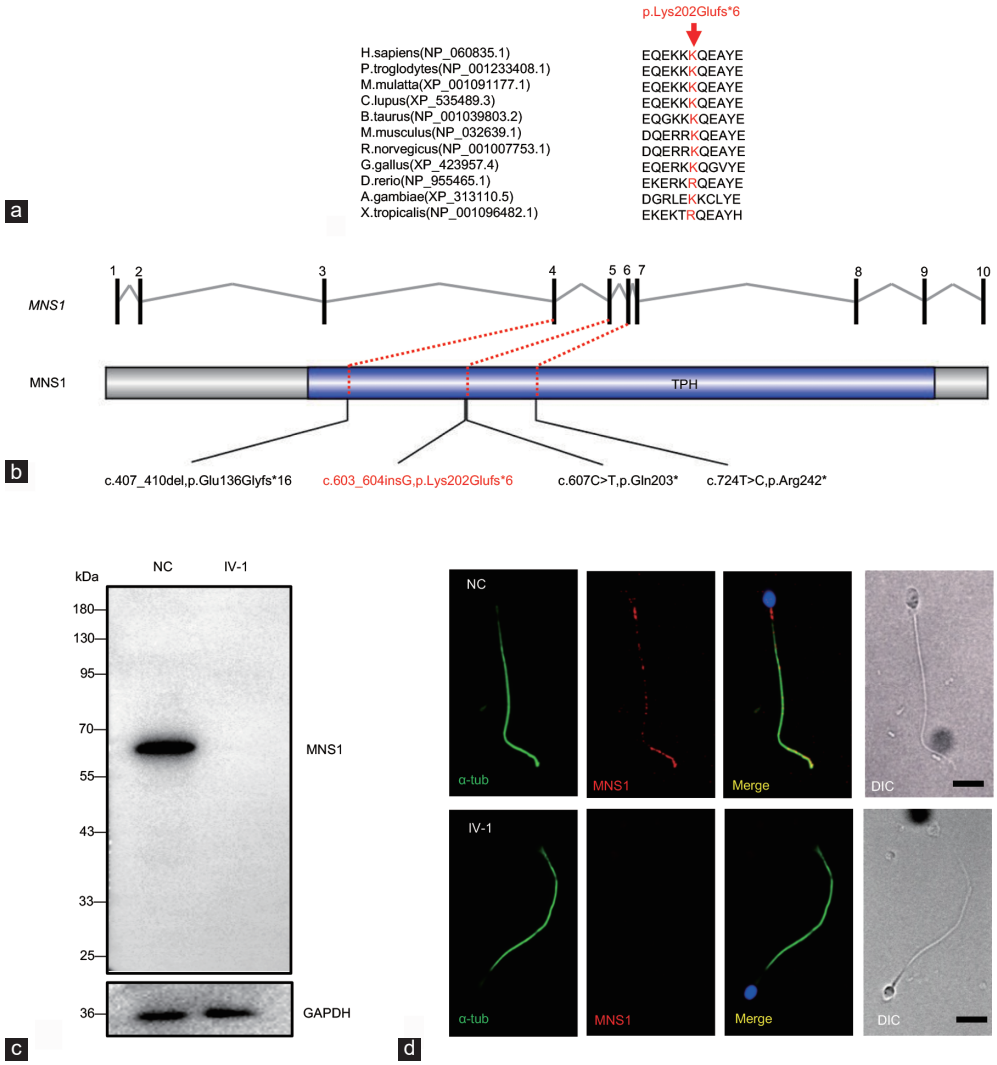

Figure 2: The impact of the *MNS1* variant. (**a**) Evolutionary conservation analysis of the *MNS1* variant among different species. (**b**) The positions of the identified variant (red) and previously reported mutations (black) in *MNS1* in patients are shown. The trichohyalin–plectin–homology (TPH) domain (http://smart.embl-heidelberg.de/) in MNS1 is indicated in blue. (**c**) Western blot analysis shows that the MNS1 protein (approximately 60 kDa) is absent from the proband's sperm. (**d**) Immunostaining analysis shows that MNS1 is localized in the flagella of the sperm in the NC, but was absent in the sperm of the proband (IV-1; $n = 120$). In the NC, the staining of MNS1 in the midpiece is prominent, whereas that in the principal and end piece is distributed discretely with distinct dots. Scale bars = 5 μm. *MNS1*: meiosis-specific nuclear structural 1; α-tub: alpha-tubulin; GAPDH: glyceraldehyde 3-phosphate dehydrogenase; NC: normal control.

Table 3: The flagellar morphology of the proband's sperm

Flagellar morphology (n=120)	*Absent*	*Bent*	*Coiled*	*Short*	*Normal*
n (%)	18 (15.0)	24 (20.0)	35 (29.2)	39 (32.5)	4 (3.3)

expression and location of markers of fibrous sheath (FS; AKAP4; **Supplementary Figure 1b**),[23] mitochondrial sheath (MS; TOMM20; **Supplementary Figure 1c**),[24] and inner dynein arms (IDA; DNALI1; **Supplementary Figure 1d**)[27] revealed no abnormalities. Taken together, these results indicate that defective MNS1 may impair the assembly of DMTs and ODAs during flagellar formation in humans.

Intracytoplasmic sperm injection (ICSI) and pregnancy outcome

The couple had undergone two ICSI cycles at another hospital in 2014. However, the first transplant failed due to implantation failure, and the second result was an ectopic pregnancy. His wife underwent laparoscopic surgery following the ectopic pregnancy to clear ovarian lesions. In 2017, it was discovered that she had endometrial polypoid hyperplasia and bilateral polycystic ovarian changes. At our hospital, 11 eggs were collected from the proband's wife in 2018, ten of which were MII oocytes and were used for ICSI with the spermatozoa of the proband. Then, eight eggs were fertilized successfully (fertilization rate: 80%), and eight viable cleavage embryos were achieved, which suggests that normal embryos could be obtained using the spermatozoa with the *MNS1* mutation during ICSI treatment. Finally, two frozen embryos were transplanted; however, the proband's wife still failed to conceive after transplantation (**Table 1**).

DISCUSSION

In this study, we identified a novel homozygous frameshift mutation in *MNS1* in a patient with severe OAT. Subsequent analysis showed morphological abnormalities in flagella and ultrastructural disturbances

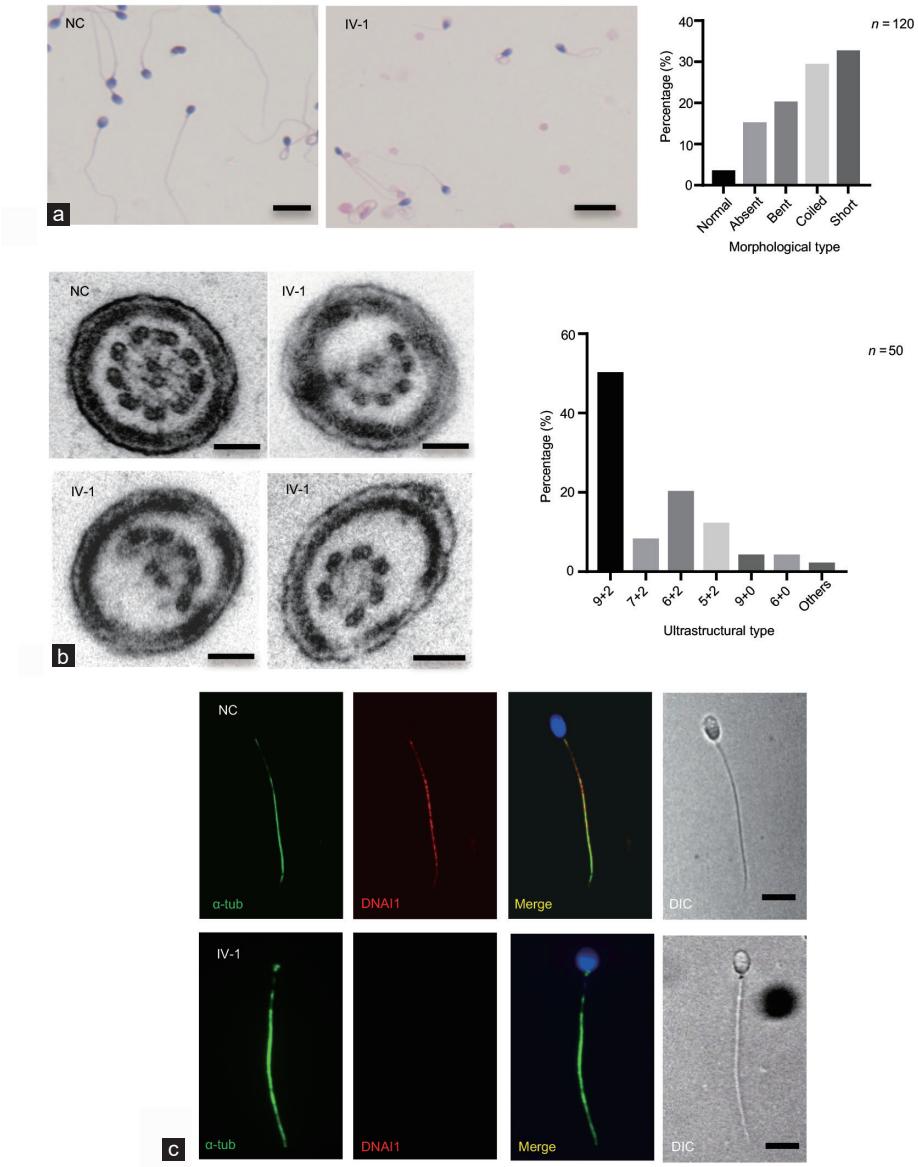

Figure 3: The morphological and structural abnormalities in the proband with *MNS1* mutation. (**a**) H&E staining shows that there were many morphological abnormalities in the proband's sperm, including absent, bent, coiled, and short flagella, compared to the NC. Scale bars = 10 μm. A histogram summary of the sperm morphology is shown on the right. (**b**) Transmission electron micrographs show subtle ultrastructural defects in the proband's sperm, with the absence of outer doublet microtubules or central pair complex of the cross-sections, compared to NC samples. A red asterisk shows the absence of central pair complex. Scale bars = 100 nm. A histogram summary of the ultrastructural defects is shown in the right. (**c**) Immunofluorescence shows the expression and location of DNAI1 (a marker for outer dynein arm). Compared to NC, DNAI1 staining appears absent from the sperm flagella in the proband (n = 120). Scale bars = 5 μm. *MNS1*: meiosis-specific nuclear structural 1; α-tub: alpha-tubulin; GAPDH: glyceraldehyde 3-phosphate dehydrogenase; NC: normal control; H&E: hematoxylin and eosin.

of axoneme in the proband's spermatozoa. MNS1 is normally located at the whole-length sperm flagella, but was almost completely absent in the proband's sperm. Overall, our study showed that loss of function of *MNS1* was responsible for the OAT phenotype of this proband and *MNS1* may play an important role during spermatogenesis.

MNS1 encodes a 495-amino acid protein, which includes the trichohyalin–plectin–homology (TPH) domain (https://smart.embl.de/smart) and five coiled-coils (http://www.ebi.ac.uk/interpro). The localization and function of MNS1 in spermatogenesis is poorly understood. During spermiogenesis, MNS1 is known to be a KIF3A-mediated cargo protein transiently transported (a motor protein) to the manchette,[30] which is a transient microtubular structure with an essential role in the transport/assembly of peri-axonemal structures. Moreover, sodium dodecyl sulfate treatment of caudal epididymal sperm indicated that MNS1 may exist in the detergent-resistant flagellar structures (peri-axoneme structures) of the sperm flagella.[17] MNS1 has also been shown to interact with a mitochondrial fusion protein, mitofusin 2 (MFN2).[31] In our study, we identified that MNS1 is localized to not only the mid and principal piece, but also the endpiece (eliminated of any peri-axonemal structures) of sperm flagella. Thus, we speculated that full-length MNS1 may also play a role in the axoneme in addition to that in the peri-axoneme of sperm flagella.

MNS1 has been shown to function in other motile cilia without peri-axonemal structures, such as ventricle and nodal cilia. In

both humans and mice, MNS1 is known to be associated with the motility of embryonic node cilia,[19] whose defect can cause random situs solitus or lateral abnormalities.[17,19] *Mns1*-knockout mice also exhibited hydrocephalus, whereas no such abnormalities have been reported in humans.[17] In the respiratory system, MNS1 was previously identified in the ciliary proteome of human bronchial epithelial cells,[16] and a few ODAs were missing in *Mns1*-deficient tracheal cilia in mice.[17] In our study, MNS1 defect was associated with missing peripheral DMTs (2–4 out of 9) and absent ODAs in humans, which is in agreement with the previous findings of a subtle ODA defect in the axonemes of respiratory epithelial cells in Israeli individuals possessing a founder homozygous nonsense mutation (c.724T>C, p.Arg242*) in *MNS1*.[19] Importantly, an ODA docking complex protein (CCDC114) has been demonstrated to interact with MNS1 and showed reduced expression when MNS1 was defective.[19] These results suggest that MNS1 is of great importance for the normal localization and assembly of axonemal structures and may play a role in ODA docking during axonemal formation. MNS1 has been demonstrated to self-dimerize in a head-to-tail fashion and is known to have different isoforms.[17] Therefore, we speculate that different isoforms of MNS1 could function with different mechanisms during spermiogenesis and ciliogenesis.

However, in our study and existing literature, *MNS1* mutations are only associated with human OAT and lateral abnormalities, but not definite respiratory disorders – the hallmark of primary ciliary dyskinesia (PCD, OMIM#2444). PCD is a heterogeneous disease characterized by recurrent infections of the respiratory system (*e.g.*, bronchiectasis and chronic sinusitis), which is caused by the defective motility of motile cilia.[32] Owing to randomization, situs abnormalities only occur in about half of the patients with PCD and can also be caused by a deficiency in other genes unrelated to PCD.[33,34] Male infertility due to flagellar defects is not included in the diagnosis of PCD.[32] Further, sperm parameters are not systematically explored in patients with PCD and are often only scarcely described during PCD-related investigations.[35] Leslie *et al.*[18] recently identified another homozygous *MNS1* Amish founder gene variant (c.407_410del; p.Glu136Glyfs*16) to be responsible for laterality defects and male infertility without other features of PCD or ciliopathies. Taken together, *MNS1* may not be a definite PCD-related gene, even though it is expressed in respiratory cilia and its function may be dispensable or complemented by other proteins. However, *MNS1* is essential for determining left–right asymmetry and flagellar biogenesis, and further investigation is needed to characterize the precise molecular role of MNS1 in cilium and flagellum biogenesis. Moreover, MMAF syndrome is also a specific type of asthenoteratozoospermia, and it has been speculated that MMAF could be a phenotypic variation of classic PCD with seemingly lighter respiratory symptoms.[36] Based on the current evidence of the flagellar morphological similarity between patients with *MNS1* mutant and those with MMAF,[37] *MNS1* may also be a causative gene of MMAF.

There have been no previously reported ICSI outcomes for patients with *MNS1* mutations. In this study, the fertilization rate of the ICSI cycle using the proband's sperm was 80%, suggesting that using the proband's sperm for ICSI could generate viable embryos. The failed transplant may be caused by the maternal factor. However, whether sperm defects caused by *MNS1* mutations could affect potential embryonic development or impair ICSI outcomes needs further investigation in a larger population, or a mouse model.

CONCLUSION

Our study demonstrated that a novel homozygous frameshift mutation in *MNS1* was responsible for OAT in a human subject. This is the first report on a Chinese OAT proband harboring a *MNS1* mutation and the results of his ICSI treatment. Our findings may contribute to the genetic counseling and fertility guidance of patients with male infertility and laterality defects.

AUTHOR CONTRIBUTIONS

YL performed the functional experiments and wrote the manuscript. WLW analyzed the WES data and helped to draft the manuscript. CFT performed the bioinformatics analysis. LLM and TYH collected the samples. JD carried out the genetic studies. GL provided clinical information. HCN and YQT conceived the study and participated in its design and coordination. All authors read and approved the final manuscript.

COMPETING INTERESTS

All authors declare no competing interests.

ACKNOWLEDGMENTS

We thank the proband in this research and his family members for their consent and support to publish this manuscript. This study was supported by grants from the National Key Science Program S&T Program (2018YFC1004900 to YQT), the National Natural Science Foundation of China (81971447 to YQT), the Science and Technology Major Project of the Ministry of Science and Technology of Hunan Province (2017SK1030 to YQT), and Graduate Research and Innovation Projects of Central South University (2019zzts734 to YL and 2019zzts322 to WLW).

Supplementary Information is linked to the online version of the paper on the *Asian Journal of Andrology* website.

REFERENCES

1 de Kretser DM. Male infertility. *Lancet* 1997; 349: 787–90.
2 Cooper TG, Noonan E, von Eckardstein S, Auger J, Baker HW, *et al*. World Health Organization reference values for human semen characteristics. *Hum Reprod Update* 2010; 16: 231–45.
3 Jungwirth A, Giwercman A, Tournaye H, Diemer T, Kopa Z, *et al*. European Association of Urology guidelines on male infertility: the 2012 update. *Eur Urol* 2012; 62: 324–32.
4 Cavallini G. Male idiopathic oligoasthenoteratozoospermia. *Asian J Androl* 2006; 8: 143–57.
5 Ben Khelifa M, Coutton C, Zouari R, Karaouzene T, Rendu J, *et al.* Mutations in *DNAH1*, which encodes an inner arm heavy chain dynein, lead to male infertility from multiple morphological abnormalities of the sperm flagella. *Am J Hum Genet* 2014; 94: 95–104.
6 Poongothai J, Gopenath TS, Manonayaki S. Genetics of human male infertility. *Singapore Med J* 2009; 50: 336–47.
7 Krausz C, Escamilla AR, Chianese C. Genetics of male infertility: from research to clinic. *Reproduction* 2015; 150: R159–74.
8 Schultz N, Hamra FK, Garbers DL. A multitude of genes expressed solely in meiotic or postmeiotic spermatogenic cells offers a myriad of contraceptive targets. *Proc Natl Acad Sci U S A* 2003; 100: 12201–6.
9 Yin H, Ma H, Hussain S, Zhang H, Xie X, *et al*. A homozygous *FANCM* frameshift pathogenic variant causes male infertility. *Genet Med* 2019; 21: 62–70.
10 Coutton C, Vargas AS, Amiri-Yekta A, Kherraf ZE, Ben Mustapha SF, *et al*. Mutations in *CFAP43* and *CFAP44* cause male infertility and flagellum defects in Trypanosoma and human. *Nat Commun* 2018; 9: 686.
11 Miyazaki T, Mori M, Yoshida CA, Ito C, Yamatoya K, *et al. Galnt3* deficiency disrupts acrosome formation and leads to oligoasthenoteratozoospermia. *Histochem Cell Biol* 2013; 139: 339–54.
12 Nakamura T, Yao R, Ogawa T, Suzuki T, Ito C, *et al.* Oligo-astheno-teratozoospermia in mice lacking Cnot7, a regulator of retinoid X receptor beta. *Nat Genet* 2004; 36: 528–33.
13 Juneja SC, van Deursen JM. A mouse model of familial oligoasthenoteratozoospermia. *Hum Reprod* 2005; 20: 881–93.
14 Fujita E, Kouroku Y, Ozeki S, Tanabe Y, Toyama Y, *et al*. Oligo-astheno-teratozoospermia in mice lacking RA175/TSLC1/SynCAM/IGSF4A, a cell adhesion molecule in the immunoglobulin superfamily. *Mol Cell Biol* 2006; 26: 718–26.

15 Udagawa O, Ito C, Ogonuki N, Sato H, Lee S, *et al*. Oligo-astheno-teratozoospermia in mice lacking ORP4, a sterol-binding protein in the OSBP-related protein family. *Genes Cells* 2014; 19: 13–27.
16 Ostrowski LE, Blackburn K, Radde KM, Moyer MB, Schlatzer DM, *et al*. A proteomic analysis of human cilia: identification of novel components. *Mol Cell Proteomics* 2002; 1: 451–65.
17 Zhou J, Yang F, Leu NA, Wang PJ. MNS1 is essential for spermiogenesis and motile ciliary functions in mice. *PLoS Genet* 2012; 8: e1002516.
18 Leslie JS, Rawlins LE, Chioza BA, Olubodun OR, Salter CG, *et al. MNS1* variant associated with situs inversus and male infertility. *Eur J Hum Genet* 2020; 28: 50–5.
19 Ta-Shma A, Hjeij R, Perles Z, Dougherty GW, Abu Zahira I, *et al.* Homozygous loss-of-function mutations in *MNS1* cause laterality defects and likely male infertility. *PLoS Genet* 2018; 14: e1007602.
20 Tan YQ, Tu C, Meng L, Yuan S, Sjaarda C, *et al.* Loss-of-function mutations in *TDRD7* lead to a rare novel syndrome combining congenital cataract and nonobstructive azoospermia in humans. *Genet Med* 2019; 21: 1209–17.
21 Seelow D, Schuelke M, Hildebrandt F, Nurnberg P. HomozygosityMapper – an interactive approach to homozygosity mapping. *Nucleic Acids Res* 2009; 37: W593–9.
22 Dai C, Hu L, Gong F, Tan Y, Cai S, *et al. ZP2* pathogenic variants cause in vitro fertilization failure and female infertility. *Genet Med* 2019; 21: 431–40.
23 Brown PR, Miki K, Harper DB, Eddy EM. A-kinase anchoring protein 4 binding proteins in the fibrous sheath of the sperm flagellum. *Biol Reprod* 2003; 68: 2241–8.
24 Lithgow T. Targeting of proteins to mitochondria. *FEBS Lett* 2000; 476: 22–6.
25 Guichard C, Harricane MC, Lafitte JJ, Godard P, Zaegel M, *et al.* Axonemal dynein intermediate-chain gene (*DNAI1*) mutations result in situs inversus and primary ciliary dyskinesia (Kartagener syndrome). *Am J Hum Genet* 2001; 68: 1030–5.
26 Sironen A, Shoemark A, Patel M, Loebinger MR, Mitchison HM. Sperm defects in primary ciliary dyskinesia and related causes of male infertility. *Cell Mol Life Sci* 2020; 77: 2029–48.
27 Mazor M, Alkrinawi S, Chalifa-Caspi V, Manor E, Sheffield VC, *et al.* Primary ciliary dyskinesia caused by homozygous mutation in *DNAL1*, encoding dynein light chain 1. *Am J Hum Genet* 2011; 88: 599–607.
28 Sanchez-Alvarez J, Cano-Corres R, Fuentes-Arderiu X. A Complement for the WHO Laboratory Manual for the Examination and Processing of Human Semen (First Edition, 2010). *EJIFCC* 2012; 23: 103–6.
29 Wang W, Tu C, Nie H, Meng L, Li Y, *et al.* Biallelic mutations in *CFAP65* lead to severe asthenoteratospermia due to acrosome hypoplasia and flagellum malformations. *J Med Genet* 2019; 56: 750–7.
30 Lehti MS, Kotaja N, Sironen A. KIF3A is essential for sperm tail formation and manchette function. *Mol Cell Endocrinol* 2013; 377: 44–55.
31 Vadnais ML, Lin AM, Gerton GL. Mitochondrial fusion protein MFN2 interacts with the mitostatin-related protein MNS1 required for mouse sperm flagellar structure and function. *Cilia* 2014; 3: 5.
32 Shapiro AJ, Davis SD, Polineni D, Manion M, Rosenfeld M, *et al.* Diagnosis of Primary Ciliary Dyskinesia. An Official American Thoracic Society Clinical Practice Guideline. *Am J Respir Crit Care Med* 2018; 197: e24–39.
33 Burdine RD, Schier AF. Conserved and divergent mechanisms in left-right axis formation. *Genes Dev* 2000; 14: 763–76.
34 Noel ES, Momenah TS, Al-Dagriri K, Al-Suwaid A, Al-Shahrani S, *et al.* A zebrafish loss-of-function model for human *CFAP53* mutations reveals its specific role in laterality organ function. *Hum Mutat* 2016; 37: 194–200.
35 Ray PF, Toure A, Metzler-Guillemain C, Mitchell MJ, Arnoult C, *et al.* Genetic abnormalities leading to qualitative defects of sperm morphology or function. *Clin Genet* 2017; 91: 217–32.
36 Coutton C, Escoffier J, Martinez G, Arnoult C, Ray PF. Teratozoospermia: spotlight on the main genetic actors in the human. *Hum Reprod Update* 2015; 21: 455–85.
37 Nsota Mbango JF, Coutton C, Arnoult C, Ray PF, Toure A. Genetic causes of male infertility: snapshot on morphological abnormalities of the sperm flagellum. *Basic Clin Androl* 2019; 29: 2.

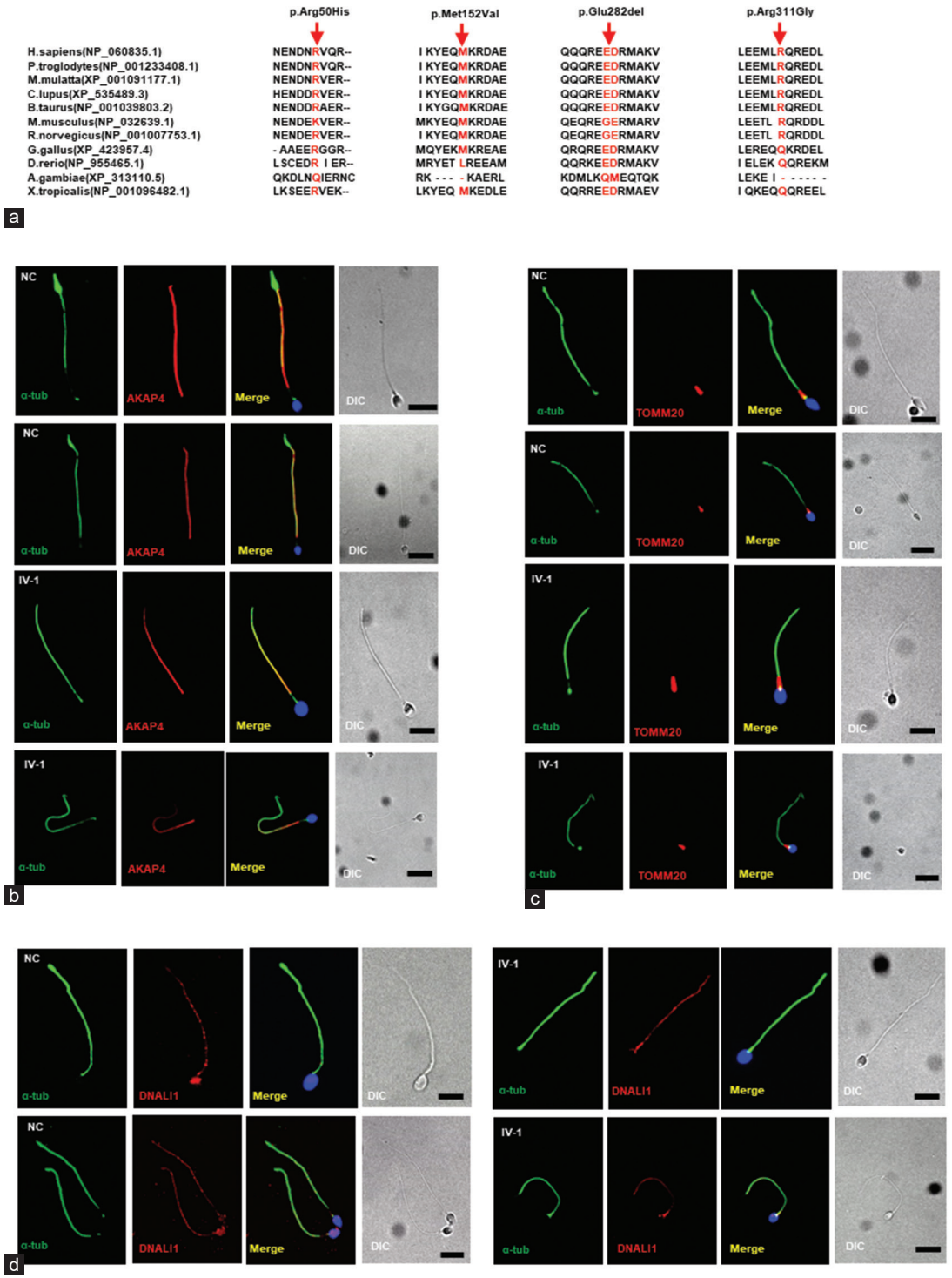

Supplementary Figure 1: The impact of *MNS1* variants. (**a**) Evolutionary conservation analysis of the heterozygous variants in *MNS1* identified in P1–P6. (**b**) Immunofluorescence shows that the expression of AKAP4 (a marker for the fibrous sheath) was present in the principal piece of the sperm in both the proband and the NC, with no differences (n = 100). (**c**) Immunofluorescence shows that the expression of TOMM20 (a marker for the mitochondrial sheath) was present in the midpiece of the sperm in both the proband and NC, with no differences (n = 100). (**d**) Immunofluorescence shows that the expression of DNALI1 (a marker for inner dynein arm) was distributed in the whole sperm flagella in the proband and NC, and its staining was consistent in both (n = 100). Scale bars = 5 μm. NC: normal control.

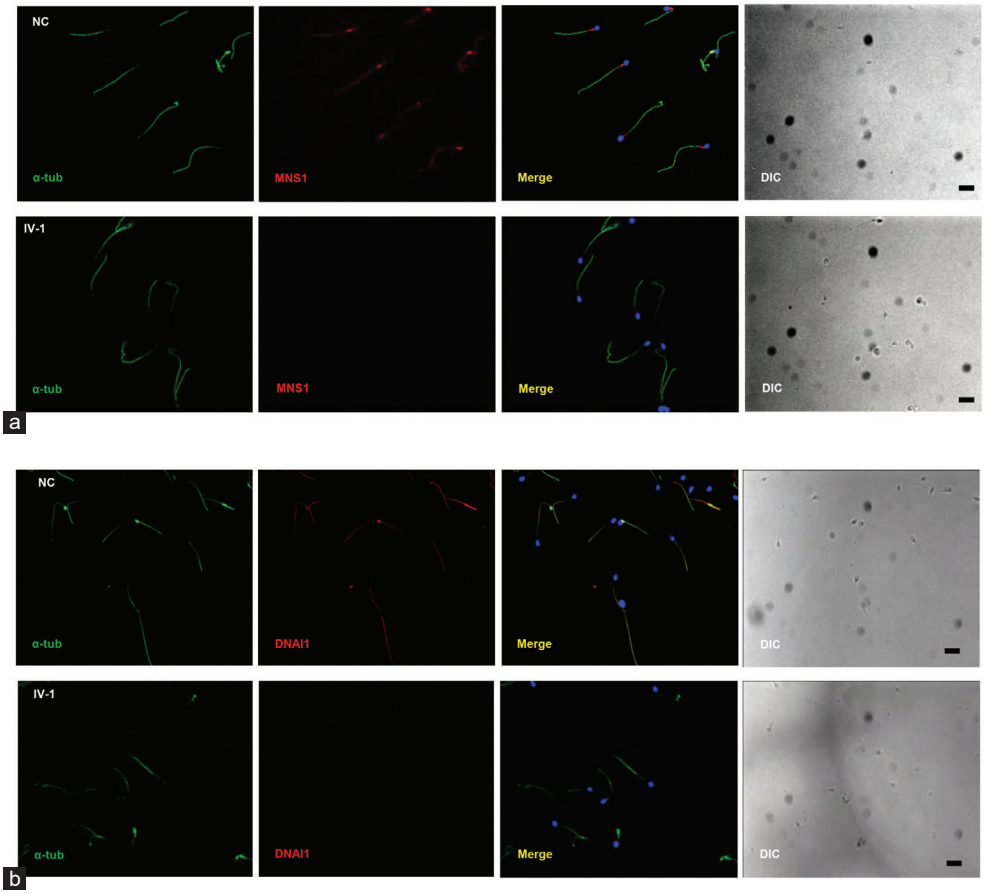

Supplementary Figure 2: Immunostaining analysis of the proband sperm. (**a**) Immunostaining analysis shows that MNS1 staining was present in the whole flagella of the NC sperm but was totally absent in the sperm of proband (IV-1) ($n = 120$). (**b**) Immunofluorescence shows that the DNAI1 staining was absent in the sperm flagella in the proband ($n = 120$). Scale bars = 5 μm. NC: normal control.

Supplementary Table 1: The information of antibodies used for immunofluorescence and Western blot

Target	*Host*	*Reference*	*Dilution*
MNS1	Rabbit	Sigma-Aldrich HPA039975	IF:1:100 WB:1:500
DNAI1	Rabbit	Bioworld BS90420	IF:1:200
DNALI1	Rabbit	Abcam ab87075	IF:1:100
AKAP4	Rabbit	Sigma-Aldrich HPA020046	IF:1:200
TOMM20	Rabbit	Proteintech 11802-1-AP	IF:1:400
α-tubulin	Mouse	Sigma-Aldrich T5168	IF:1:1000
Dylight 488 goat anti-mouse IgG	Goat	Invitrogen	IF:1:400
Dylight 555 goat anti-rabbit IgG	Goat	Invitrogen	IF:1:400
GAPDH	Mouse	Abcam ab8245	WB:1:2000
Horseradish peroxidase -conjugated anti-mouse IgG	Goat	MultiSciences GAM007-100	WB:1:5000
Horseradish peroxidase -conjugated anti-rabbit IgG	Goat	MultiSciences GAR007-100	WB:1:5000

Supplementary Table 2: Primers used in Sanger sequencing of meiosis-specific nuclear structural 1 heterozygous variants

Patient	*Variant*	*Primer*	*Primer sequences*	*Exon*	*Product size*
P1/P2	c.G149A	Forward	ATCGTAGGGTTCCAAAAGGAG	2	384
		Reverse	CCCAGGTCTTTACGATTACACC		
P3/P4	c.A454G	Forward	CCGCTGTATTCCCTCTTTGAGTA	4	429
		Reverse	TGGTCATTCTAAGCAGCAATGT		
P5	c. 846_848del	Forward	CTGTACTTGTTATTGCTTTTCAGGG	6	414
		Reverse	TCCTGGTATAATTCTTGTCGCAC		
P6	c.G932A	Forward	AATGAATGCAATGCGAAGGT	7	441
		Reverse	CTTCTCTACATTAATCATTCTTTCC		